



Technical note: apatite and zircon (U-Th)/He analysis using quadrupole and magnetic sector mass spectrometry

5 Cécile Gautheron¹, Rosella Pinna-Jamme¹, Alexis Derycke¹, Floriane Ahadi¹, Caroline Sanchez¹,
Frédéric Haurine¹, Gael Monvoisin¹, Damien Barbosa¹, Guillaume Delpech¹, Joseph Maltese², Philippe
Sarda¹, Laurent Tassan-Got²

¹Université Paris-Saclay, CNRS, GEOPS, 91405, Orsay, France

²Université Paris-Saclay, CNRS/IN2P3, IJCLab, 91405 Orsay, France

Correspondence to: Cécile Gautheron (cecile.gautheron@universite-paris-saclay.fr)

10 **Abstract.** Apatite and zircon (U-Th)/He thermochronological data are obtained through a combination of crystal selection, He
content measurement by extraction from crystal and analysis using noble gas mass spectrometry, and measurement of U, Th
and Sm contents by dissolution and solution analysis using inductively coupled plasma mass spectrometry (ICP-MS). In this
contribution, we detail the complete protocols developed for over more than a decade that allow apatite and zircon (U-Th)/He
data to be obtained with precision. More specifically, we show that the He content can be determined with a high precision
15 using a calibration of the He sensibility based on the Durango apatite and its use also appears crucial to check for He, U-Th-
Sm analytical problems. The Durango apatite used as a standard is therefore a suitable mineral to perform precise He calibration
and yield (U-Th)/He ages of 31.1 ± 1.4 Ma with an analytical error of less than 5%. The (U-Th)/He ages for the FCT zircon
standard yields a dispersion of about 9%, with mean age of 27.0 ± 2.6 Ma comparable to other laboratories. For the long-term
quality control of the (U-Th)/He data, attention has been paid to evaluate the drift of He sensibility, blanks through time and
20 those of (U-Th)/He ages and Th/U ratios (with Sm/Th when possible), all associated with the use of Durango apatite and Fish
Canyon Tuff zircon as standards.

1 Introduction

Apatite and zircon (U-Th)/He (AHe and ZHe respectively) thermochronology is now a mainstream tool to reconstruct
the Earth evolution (e.g. Farley, 2000; Farley, 2002; Gautheron and Zeitler, 2020; Reiners, 2005; Reiners and Brandon, 2006).
25 The geological implications of these data rely on the precision of measurements of He, U, Th and Sm contents of apatite and
zircon crystals, by: (i) crystal picking; (ii) non-destructive He degassing and content determination by mass spectrometry; (iii)
U, Th and Sm analysis after crystal dissolution and solution analysis by ICP-MS. Different contributions have already
presented parts of the analytical protocols, for example, He degassing using laser beam (e.g. Foeken et al., 2006; House et al.,
2000), dissolution and analysis of U, Th, Sm, Ca or Zr (e.g. Evans et al., 2005; Guenther et al., 2016; Reiners and Nicolescu,



2007) or improvements of the noble gas analysis by magnetic sector mass spectrometry (Burnard and Farley, 2000). In this contribution, we aim to present all the developed and used methodologies, focused on He degassing and He content analysis, dissolution, ICP-MS analysis and data reduction that lead to (U-Th)/He thermochronological data. Specifically, analytical details are given on two homemade noble gas extraction-purification lines that are coupled either to a quadrupole mass spectrometer for one or a magnetic sector mass spectrometer. An inexpensive method of He content calibration using the Durango apatite crystals standard is presented. Finally, (U-Th)/He data obtained in the laboratory for Durango apatite and Fish Canyon Tuff (FCT) zircon over a period of 6 to 8 months are presented. The results allow discussing about data acquisition, analytical difficulties and the He, U, Th (Sm for apatite) contents and (U-Th)/He data reproducibility.

2 Methods

2.1 Apatite and zircon samples preparation, picking and packing

Apatite and zircon crystals are extracted from plutonic or sedimentary rocks by classical crushing methods, sieved (mesh < 400 μm), and separated following density (tribromomethane and di-iodomethane – VWR®) and magnetic (L-1 Frantz Isodynamic® Separator) methods. For Durango apatite gem crystal, a gentle crushing into an agate mortar allows getting fragments of different sizes. Inclusion-free automorphic apatite and zircons or Durango apatite fragments are picked under a binocular microscope (SZX12 – Olympus) and selected as a function of fragment size (>60 μm). For an automorphic crystal, the length, height and width are measured, and the termination geometry of the crystal (broken faces, pyramids, no pyramids) are recorded. Ejection factor (F_T) and equivalent sphere radius (R_s or named also ESR) are determined using the Monte Carlo simulation of Gautheron and Tassan-Got (2010); Gautheron et al. (2012) and Ketcham et al. (2011). As the ejection length for the Th decay chain is higher than that for the U decay chains, the value of Th/U ratio is fixed to the measured value to avoid over or under- corrections (Ketcham et al., 2011; Ziegler, 2008). An internal modification of the Monte Carlo simulation (QTLFT software), coupled with an excel automatic file generation, is used to calculate the F_T , R_s and crystals weight from a list of different crystals geometries.

Each apatite and zircon crystal or fragment were placed respectively into a platinum tube (99.95% purity, 1.0×1.0 mm – Johnson Matthey®) or a niobium tube (purity 99.95%, 1.0×1.0 mm – Alpha Aesar®). The choice of the capsule (Nb, Pt) for



packaging is strictly related to the acid attack protocol. During U, Th and Sm analysis by means of ICP-MS instruments, the
55 presence of Pt⁺ ions at high concentration (>320 µg/ml) in the sample solution may lead to the formation of complex, platinum
argides ¹⁹⁴Pt⁴⁰Ar⁺, ¹⁹⁵Pt⁴⁰Ar⁺, ¹⁹⁸Pt⁴⁰Ar⁺, that cause isobaric interferences with the measured U isotopes at masses 234, 235 and
238 (Evans et al., 2005; Reiners and Nicolescu, 2007). Apatite chemical digestion can be achieved using acid digestion at low
concentration (HNO₃ 5N ultra-pure) and low temperature (65°C), is not able to dissolve the capsule, therefore Pt tubes can be
used. However, an acid digestion method using concentrated acids is instead adopted for zircon (HCl and pure HF 27N) at
60 high temperatures (220°C), which leads to a total dissolution of the Pt capsule, therefore, Nb tubes were adopted instead.
Although niobium-argon complexes do not create isobaric interferences with the analyzed U masses, the solution, highly
concentrated in Nb may, however, cause a partial precipitation of the uranium and thorium (Evans et al., 2005).

2.2 Helium analysis protocol

The helium content analyses were performed at GEOPS laboratory, Paris Saclay University (Orsay, France). Each capsule
65 containing a crystal, fragments, or grain(s) was degassed using either a homemade He extraction line coupled with a quadrupole
mass spectrometer (Prisma QMG 100 Pfeiffer©), further referred to as the He line, or another homemade line connected to a
rehabilitated VG5400 magnetic sector mass spectrometer, further referred to as the VG line. The He and VG lines are fully
automated using LabView Std, from the heating phase to the helium analysis. Each portion of the line is divided into sections
(extraction, purification, analysis) by pneumatic Swagelok© valves coupled to electro-valves (E.V 3/2 NF Direct Flasque.D2,4
70 ALU BUNA, TH France) and activated by pressurized air. Ultra-high vacuum conditions (<10⁻⁹ mbar) are guaranteed by using
a system of turbomolecular (HighCube – Pfeiffer SAS©) and ionic pumps (StarCell – Varian©). Figure 1 presents the
schematic geometry of the two homemade He and VG lines, with the different parts that are controlled using LabView.

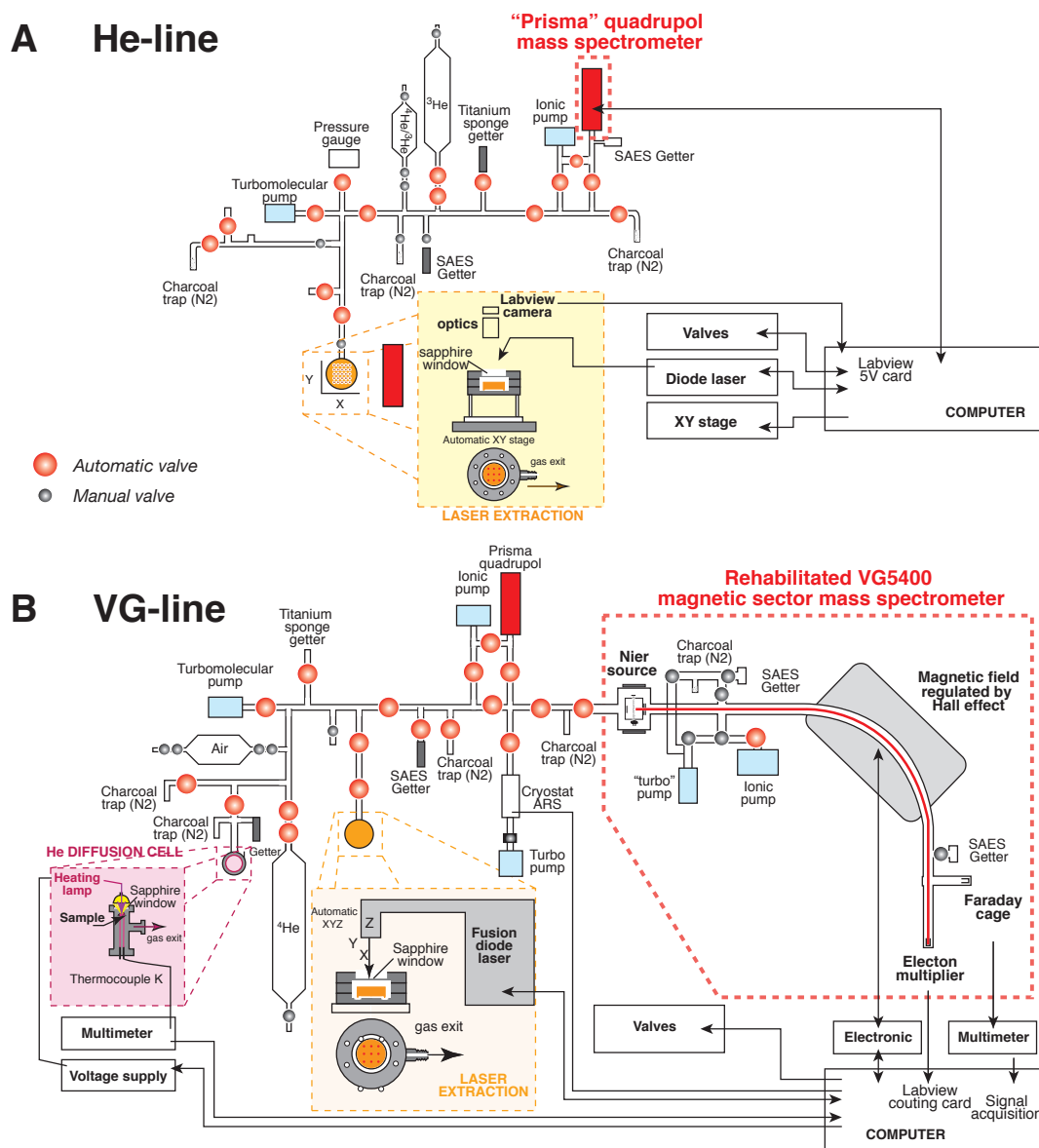


Figure 1: Schematic representation of the homemade systems for He extraction, purification and analysis by mass spectrometer: (A) He line and (B) VG line.

Platinum and niobium tubes adopted for sample packaging are suitable because of the low hydrogen they release at high vacuum, their malleability and their U, Th, Sm and REE purity. Being metallic materials, they ensure a homogeneous heat transfer during laser shooting. For the He line, the Pt/Nb tubes are deposited on a copper planchette containing 25 or 49



80 positions and are placed into a cell that moves in front of the laser beam using a X-Y motor system (SMC100CC – Newport
 ©) controlled by LabView. An Ytterbium doped infra-red diode laser coupled with an optic (wavelength 1064 nm – 1080 nm,
 10W ManLight; Laser2000), placed at a focal distance of 4 cm from the sample, allows heating up the capsules with a beam
 of 70 μ m diameter. For the VG line, the Pt/Nb tubes are placed on an inox or copper planchette containing 12 or 49 positions
 and the heating is ensured using an infrared diode fusion laser (Teledyne, USA) moving in front of the cell. After each sample
 85 loading, the line (He and VG line) is heated overnight at low temperature (<50°C) to remove any gas absorbed on the inner
 walls of the lines. In addition, ultra-high vacuum can be quickly obtained by heating an empty capsule placed in the planchette
 in order to remove air absorbed on the copper/inox planchette. Copper or inox were selected for planchette material due to
 their good thermal conductivity and their inertia in vacuum conditions. The cell is sealed with a CF63 sapphire window
 (Caburn) allowing a good transmission of the whole IR laser beam. Each capsule is heated using the heating protocol
 90 summarized on Table 1.

Table 1: samples packing and He purification and analysis protocols

Minerals	Packing	Degassing	Purification	Mass spectrometer	Standard
Apatite	Pt tube	5 min at 1050°C	Liquid N ₂ active charcoal + SAES 701 10 min	Prisma quadrupole: H ₂ , ³ He, ⁴ He, mass 5, H ₂ O, ⁴⁰ Ar, CO ₂ Electron multiplier 850 V	Volcanic Durango apatite 31.02±1.01 Ma; McDowell et al. (2005)
Zircon	Nb tube	30 min at >1250°C	Liquid N ₂ active charcoal + SAES 701 10 min	VG5400: ⁴He Electron multiplier 3500 V + LabView counting system	Volcanic Fish Canyon zircon 28.5±0.06 Ma; Schmitz and Bowring (2001)



The heating scheduled procedure was repeated on each sample until all ^4He was degassed giving a signal back to the
95 background level. The sample temperature achieved using the laser of the He line is recorded by means of a LabView camera
and a homemade algorithm that converts the total red, green and blue visible light into a temperature. We used the light
emission in visible light associated with black body light emission during heating. For this aim, a Pt capsule has been heated
with increasing values of the laser intensity and pictures have been taken at different temperature settings, as presented in
Figure 2A. At the same time, the temperature of the heated capsule has been measured using an external filament extinction
100 pyrometer. This type of pyrometer is currently used to calibrate TIMS filament temperatures. For each recorded picture, a
simple image treatment has been realized using LabView in order to retrieve the red, blue and green value on the RGB
colorimetric coding system that ranges from 0 to 255 (Fig. 2B). As the red signal is already saturated when the capsule is
emitting visible light, we chose to sum the RBG signal of the three colors, as shown on Figure 2C. The obtained RBG is
correlated with the temperature of the heated capsule. The simple image treatment procedure has been calibrated from 950 to
105 1150°C for a fixed value of the exposure time of 500 ms. The same heating calibration has been automatically applied to each
heated capsule, with an estimated error of $\pm 20^\circ\text{C}$ on temperature calculation.

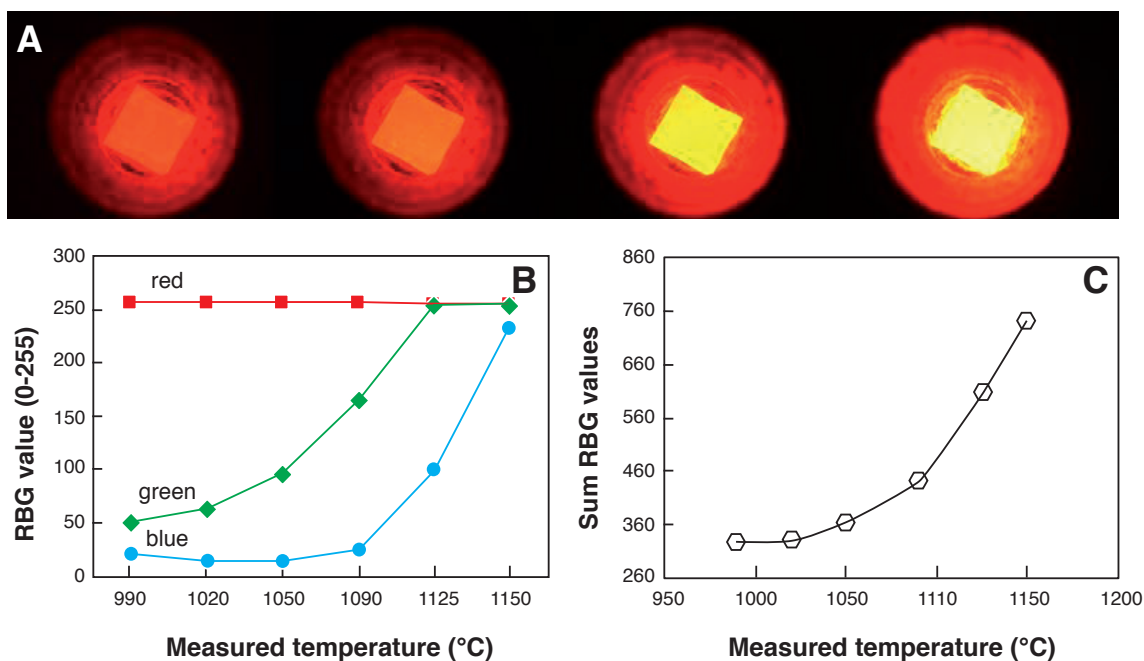


Figure 2: temperature calibration procedure of the heated capsule in visible light. **A)** Example of heated capsules with different laser beam intensities showing the change in color. **B)** and **C)** Evolution as a function of the measured temperature using a pyrometer of the RGB code values and sum of the RGB values, respectively.

The analysis protocols differ as a function of the type of mass spectrometer used and the type of analyzed minerals.

2.2.1 Helium line

115 The diffused ^4He gas is mixed with a known amount of ^3He in the purification line, used as a spike, in concentration of about 100 to 1000 times higher than the ^4He to be determined. A ~ 4000 cc (cubic centimeter) cylinder (V1), filled by ^3He gas, is connected to a pipette made by two welded valves with a small, 5 mm diameter, stainless steel cylinder placed inside to reduce the volume of the pipette (Fig. 1). The approximate volume of the pipette is ~ 0.5 cc (V2) and allows an ^3He amount of 10^{-9} to 10^{-10} ccSTP (cubic-centimeters-at-standard-temperature-and-pressure) to be introduced into the line. The amount of ^3He decreases in the cylinder by a factor of ~ 0.9999 ($V1/(V1+V2)$) for every shot of gas extracted, therefore the number of pipettes taken is automatically recorded to take the decrease of ^3He in the cylinder into account. These statistics allow the data for He age computation to be calculated with the right amount of ^3He spike introduced into the line. According to the spike conditions

120

reported above (^3He in concentration of about 100 to 1000 times higher than ^4He), it has been observed that the He line can perform a total of about 6000 analyzes.

125 The sample gas is purified from most of the H_2O , CO_2 , H_2 , Ar gases using two liquid nitrogen-cooled traps of activated charcoal, a ST707 and a ST701 SAES getter, according to different purification protocols adapted for various minerals (Table 1). The use of a hot ($>850^\circ\text{C}$) titanium sponge getter is dedicated to minerals with high CO_2 or H_2O contents. The access to the entire system of traps, individually connected to the line by means of ultra-high vacuum valves (Fig. 1), allows the analysis of a large variety of minerals containing variable abundances of CO_2 or H_2O such as calcite or goethite (Allard et al., 2018; 130 Cros et al., 2014). Beside helium isotopes (^3He and ^4He), H_2O , CO_2 , H_2 and Ar gases are additionally measured on the electron multiplier of the Prisma QMG 100 Pfeiffer quadrupole mass spectrometer to check for the effective purification of the analyzed gas. Such measurements of the gas are repeated 16 times and a linear regression of the data for the $^4\text{He}/^3\text{He}$ ratio is then calculated and includes a correction of the HD^+ isobaric contribution on the ^3He signal, even if this contribution is insignificant compared to the ^3He spike signal. In addition, we also observe that the signal at mass 4 slightly increases when the H_2 signal 135 is higher, which we interpret as either a double H_2 molecule having an isobaric impact on mass 4 or the tail of the H_2 peak having an influence on the shape of the mass 4 peak. This effect is not negligible for the low ^4He signals of typical samples, but an adapted H_2 purification protocol allows to remove this effect: a 707 SAES getter unit is positioned in the quadrupole mass spectrometer (Fig. 1).

The gas purification protocol ensures to get a close to constant (although slightly decreasing) total pressure in the line 140 and in the quadrupole mass spectrometer. The ^4He concentration is calculated using the ^3He content such as:

$$4_{\text{He}} = \left(\left(\frac{^4\text{He}}{^3\text{He}} \right)_s - \left(\frac{^4\text{He}}{^3\text{He}} \right)_b \right) \times 3_{\text{He}} \quad (1)$$

with $(^4\text{He}/^3\text{He})_s$ and $(^4\text{He}/^3\text{He})_b$ the ratios measured for the sample and blank respectively. The ^3He content is determined using the following equation:

$$3_{\text{He}} = \times 3_{\text{He}_c} \times \left(\frac{V_1}{V_1+V_2} \times D \right)^N \quad (2)$$

145 V_1 is the volume of the ^3He cylinder (~ 4000 cc), V_2 the pipette volume ($\sim 0,5$ cc) and N the pipette number (i.e. N is the number of introductions of the pipette volume). $^3\text{He}_c$ is the ^3He content value adapted for each calibration and D is the ‘drift’,

an additional parameter introduced allowing to take into account the evolution of sensitivity of the quadrupole mass spectrometer along with external parameters such as temperature or even power failures. D acts as if the pipette volume V_2 could vary to mime the variations of the quadrupole sensitivity. D is determined manually and changes according to the

150 Durango standard results, especially every time the source is tuned again. The product $3_{He_c} \times \left(\frac{V_1}{V_1+V_2} \times D\right)^N$ thus decreases regularly and homogeneously.

2.2.2 VG line

The diffused ^4He is purified from the H_2O , CO_2 , H_2 , Ar gases using two ST707 SAES-getters and a Ti sponge getter (Fig. 1B). A cryogenic trap from Advanced Research Systems (ARS)©, installed more recently, has the capacity to cool activated charcoal down to 8 K. At this temperature He is efficiently trapped, then further released into a smaller volume at about 50 K. Again, according to the nature of the sample to be analyzed, different purification protocols are adopted (Table 1). Every protocol is fully automatized and the ^4He gas is introduced into the VG5400 magnetic sector mass spectrometer. The filament amperage is fixed at a compromising value ranging from 300 to 400 μamps , lower than the recommended value for He analysis but ensures a longer life of the filament. Isotope ^4He is analyzed using a Pfeiffer electron multiplier (17 dynodes) which is
160 connected to an Ortec discriminator and a LabView counting card. 20 analyzes of the ^4He signal integrated over 1 sec are performed and the mean ^4He signal is recorded. The linear regression over the 20 measurements allows us to get a mean signal and the associated standard deviation. The dead time of the electronic chain is close to the width of the signal delivered by the electron multiplier which is a few ns. The maximal recorded counting rate being about 3×10^5 c/s, the dead time correction is always lower than 1% and it is neglected. The system sensitivity is determined using an internal ^4He standard from a ~ 4000 cc
165 cylinder calibrated over the Durango apatite analyses. The ^4He concentration is computed using

$$^4_{He} = (4_{He_s} - 4_{He_b}) \times s \quad (3)$$

with $^4\text{He}_s$ and $^4\text{He}_b$ are the signal for the sample and blank respectively and s the sensitivity (He/cps; cps: counts per second).

Durango apatite fragments and/or Fish Canyon Tuff zircon crystals are analyzed regularly (1 Durango/Fish Canyon
170 standard analyzed every 7 unknown samples) to check the (U-Th)/He analysis reproducibility.



2.3 Digestion chemistry protocol

2.3.1 Vessel cleaning

For apatite, we used single-use 4 ml polypropylene (PP) snap-cap tubes (supplier VWR) that do not need prewashing for our purpose. For zircon, the dissolution is made in 350 μ l PFA (PerFluoroalkoxy Teflon) parrish style vials (Savillex SAS) placed into a high pressure-high temperature dual wall digestion vessel. Before their use for acid digestion, the vials undergo a series of acid baths in a 250 ml beaker (borosilicate glass - VWR) placed on a hot plate at 100°C, according to the following sequence: cycle 1: 24h bath in diluted 5% Extran MA 02 (Merk) in MilliQ water (Milli-Q® HX 7000 SD); cycle 2: 24h bath in HCl 5N (Emsure 32% - VWR); cycle 3: 24h bath in HCl/HNO₃ 3/1 (HCl Emsure 32% VWR; HNO₃ Emsure for analysis 65% VWR); cycle 4: 24h bath in HNO₃ 5N (Emsure 65% VWR) (Table 2). Between each bath, vials are rinsed with MilliQ water (18 M Ω Direct 8 System – Merck Millipore). Vials are finally dried in an oven at 50°C and stored in a hermetically closed PP box until further use.

The degree of cleanness after the series of baths is checked by analysis of ²³⁸U, ²³²Th natural isotopes intensities and spike isotopes ²³⁰Th and ²³⁵U. The tests were carried out by filling 200 μ l MilliQ water in cleaned vials, refluxed for 2h at 100°C, and transferred to PP tubes with the addition of 800 μ l MilliQ water.

2.3.2 Samples digestion protocol

After degassing, each Pt/Nb-conditioned sample is transferred from the planchette into a vial for grain dissolution by acid digestion. The sample digestion is carried out by adding a volume of 50 μ l of a spike solution in each vial (in HNO₃ 5N and containing a known amount of ²³⁵U, ²³⁰Th - plus addition of ¹⁴⁹Sm and ⁴²Ca for apatite). According to the nature of the sample, a specific dissolution protocol may be followed (acids and heating temperature) (Table 2).

Table 2: Cleaning chemistry and chemistry protocols for prepared solution

Mineral	Vial type	Cleaning protocol	Spikes	Dissolution protocol	Solutions
Apatite	4 ml single use PP tube	No cleaning needed	50 μ l (²³⁵ U ~4 ppb; ²³⁰ Th ~4	+ 50 μ L of 5N HNO ₃ and heating for 3 h at 65°C.	Blk: acid blank



			ppb, ^{149}Sm ~4 ppb; ^{42}Ca ~800 ppb)	+ cooling time (30 min) + 1.9 ml 1N HNO_3	Blk-ch: acid blank chemistry
Zircon	350 μl PFA tubes + PFA container + stainless steel digestion bomb + oven + 4 ml single use PP tube	PFA vials: on a hot plate at 100°C: Extran 5% bath (24h); HCl 5N Emsure bath (24h); HCl: HNO_3 (1:3) Emsure bath (24h); HNO_3 5N Emsure bath (24h)	100 μl (^{235}U ~40- ^{55}ppb ; ^{230}Th ~15-20 ppb)	Step 1: Vial: +200 μL HF 27N + few drops HNO_3 7N vessel: 10 ml HF 27N + 1 ml HNO_3 7N oven: 220 °C for 96h Step 2: Evaporation at 100 °C Step 3: Vial: + 300 μL HCl 6N; Vessel: 12 ml HCl 6N; Oven: 220°C for 12h Step 4: Evaporation at 100°C Step 5: Add 200 μL HNO_3 1N + some drops HF 0.1N; 1h reflux at 100°C Step 6: Transfer to PP vial, add 800 μL HNO_3 1N Step 7: dilution 1/10 with HNO_3 1N	BSP: spiked blank BSP-ch: spiked blank chemistry BSP-ch-Pt: spiked blank chemistry with a Pt capsule for apatite BSP-ch-Nb: spiked blank chemistry with a Nb capsule for zircon DUR: natural Durango Sp: spiked sample including standard



For apatite, the dissolution protocol has been adapted from Farley (2002). The dissolution requires a soft acid digestion (HNO₃ 5N – bidistilled from HNO₃ 65– Normapur - VWR) performed in a 4 mL single-use polypropylene tube (VWR) by adding 50 μL of spike (~4 ppb of ²³⁵U, ²³⁰Th, ¹⁴⁹Sm and ~800 ppb ⁴²Ca) and 50 μl of HNO₃ 5N. The tube is then placed on a hot plate at 65°C during 3 h for digestion. After digestion, samples are diluted with 1.9 ml of HNO₃ 1N and stored at 4°C before ICP-MS analysis (Table 2). Due to the digestion conditions (using diluted acids), the Pt capsule does not dissolve and does not interfere during ICP-MS analysis. Sample digestion is always made with freshly diluted nitric acid by addition of MilliQ water. To minimize possible source contaminations from the environment, storing tubes, evaporation, ICP-MS analysis is programmed within a few days of sample digestion. After analysis, the Pt capsules are promptly collected, cleaned and sent back to the factory company in a recycling/reselling loop contract.

For zircon, the dissolution protocol was slightly adapted from Reiners (2005) and Reiners and Nicolescu (2007). The dissolution is performed in 350 μl PFA Parrish style vials (Savillex SAS). Zircons are first spiked with 100 μL of ²³⁵U and ²³⁰Th (~45 to ~55 ppb of ²³⁵U, ~15 to ~20 ppb of ²³⁰Th; Table 2). The vials are then placed into a digestion vessel hermetically sealed with a metallic gasket (IN/PFA OUT/Stainless steel PA4748, Parr Instrument Company) to hold high pressures. The digestion follows several steps summarized in Table 2. Step 1: inside the vials: addition of 200 μL HF 27N (Suprapur® – VWR) and few drops of HNO₃ 7N (Suprapur® – VWR); inside the digestion vessel: addition of 10 ml HF 27N and 1 mL of HNO₃ 7N. Once sealed, the vessel is heated up at 220°C and held at high pressure for 96 hours. Step 2: the acid solution is evaporated to dryness by placing the vials on a hot plate at 100°C. Step 3: 300 μL HCl 6N (Suprapur® – VWR) are added to each vial, the Parr vessel is filled with 12 ml HCl 6N, sealed and heated back at 220°C, under pressure for 24 hours in an oven. Step 4: the vials are evaporated to dryness on a hot plate at 100°C. Step 5: a reflux is carried out with a combination of HNO₃ 5N (200 μL) and HF 0.1 N (few drops) at 100°C for 1 hour. Step 6: the solutions are transferred to 4 ml polypropylene tubes where 800 μL HNO₃ 1N are added. Step 7: a final dilution (1/10) is done with freshly prepared HNO₃ 1N in a second 4 mL PP single-use tube. The solutions are stored at 4°C before isotopic analysis. To avoid pollution released from the storage tubes or changes in concentration by evaporation of the solutions, the ICP-MS session is always scheduled within a few days after samples dissolution.



In addition to the apatite and zircon samples, the following solutions are also prepared as summarized in Table 2; spiked sample (Sp), including Durango and FCT standards samples; acid blank (Blk): to check acid purity and potential contaminations of tubes; chemistry acid blank (Blk-ch): to check the enrichment contamination in acid caused by the chemistry protocol; spiked blank (BSP): a weighted volume of spike is added to a volume of acid in order to check variations in concentration of the spike and to take into account the contribution of natural isotopes contained in the spike; spiked blank chemistry (BSP-ch): a volume of spike in acid undergoes the same dissolution protocol than the samples, which allows to quantify contamination coming from contingencies during the dissolution protocol (vessel, user, acid); Durango solution (DUR): a single fragment of Durango is dissolved in a volume of acid, no spike is added, which allows the natural isotopic ratio the uranium to be measured for checking, as it has to be in isotopic equilibrium with $^{235}\text{U}/^{238}\text{U}=0.00725$.

2.4 Spike solution composition and calibration

As reported above, for every sample to be analyzed and according to the isotopic dilution method, a volume of 50 μl of the spike solution MR2 is introduced into the vial before the dissolution protocol. The spike solution is prepared (60 ml) every 6 to 12 months from elemental mother solutions MR1 and MR (Table 3), these being obtained from certified concentrated mono-elemental solutions: ^{235}U (10 ml, IRRM-50, 4.2543(11) nmol $^{235}\text{U}\cdot\text{g}^{-1}$, JRC - Belgium), ^{230}Th (5 ml, IRRM-61, 2.474(18) nmol $^{230}\text{Th}\cdot\text{g}^{-1}$, JRC - Belgium) and ^{149}Sm (10 ppm, 90%, 100 ml, 47,01 nmol $^{149}\text{Sm}\cdot\text{g}^{-1}$, Berry and Assoc - USA). For apatite analysis, ^{42}Ca (97.8%, Buy Isotope - Sweden) is added. Detention of JRC materials is authorized under Laboratory License for Radioactive Materials (RMs). Other isotopes, such as ^{233}U or ^{229}Th , are also available as isotopic spikes at JRC; however, their high cost due to the radioactive nuclear materials transport fees is not negligible; for this reason, we chose to use isotopes ^{235}U and ^{230}Th . In over ten years of research at the GEOPS laboratory, 16 solutions of spike for apatite and 3 solutions of spike for zircon have been produced. Since the early development of the (U-Th)/He dating method at GEOPS, other isotopes such as ^{149}Sm and ^{42}Ca were recently added to the protocol. For zircon, the addition of the isotope ^{149}Sm into the Zr-spike solution was discarded due to the negligible impact of the He budget associated with ^{147}Sm decay, compared to the He production from ^{238}U and ^{232}Th .

Before use, the spike solution MR2 is calibrated using a series of weighted solutions, obtained by mixing a volume of a mono-elemental standard solution with a volume of spike (MR2). The U_{SS} solution contains ^{238}U mono-elemental solution at



1015 ppm (99.96%, Analab France) mixed with ^{235}U spike; the Th_{SS} solution contains ^{232}Th mono-elemental solution at 993 ppm (99.93%, Analab France) mixed with ^{230}Th spike; the Sm_{SS} solution contains natural Sm 1006 ppm ($^{147}\text{Sm} = 14.99\%$, $^{149}\text{Sm} = 13.82\%$, Analab France) mixed with ^{149}Sm spike and the Ca_{SS} solution contains natural Ca at 1003 ppm ($^{42}\text{Ca}=0.65\%$, $^{43}\text{Ca}=0.13\%$, Analab France) mixed with ^{42}Ca spike (Table 3). These solutions are then analyzed by ICP-MS in order to properly calibrate the MR2 spike solution.

Table 3: U, Th, Sm and Ca spike calibration

Comment	Isotope	Volume	Solutions
Spike solutions preparation			
MR: concentrated mono-elemental mother solution and solid	$^{235}\text{U}_{\text{MR}}$	10 ml	HNO_3 5N 1 ppm (solution)
	$^{230}\text{Th}_{\text{MR}}$	5 ml	HNO_3 5N 0.56 ppm (solution)
	$^{149}\text{Sm}_{\text{MR}}$	100 ml	HNO_3 5N 10 ppm (solution)
	$^{42}\text{Ca}_{\text{MR}}$	10 ml	2.44 mg CaCO_3 (solid)
MR1: first-dilution mother spike solution obtained by dilution from the concentrated mother solution or solid (MR)			No need to prepare ^{235}U and ^{149}Sm (already at adapted concentration)
	$^{230}\text{Th}_{\text{MR1}}=100$ ppb	10 ml	2 ml $^{230}\text{Th}_{\text{MR}}$ +8 ml HNO_3 5N
	$^{42}\text{Ca}_{\text{MR1}}=1000$ ppm	10 ml	2.44 mg CaCO_3 (solid) in 10 ml HNO_3 5N
MR2: second-dilution mother spike solution obtained by mixing dilution of the concentrated (MR) and first-dilution mother spike (MR1)	$^{235}\text{U}_{\text{MR2}}=4$ ppb $^{230}\text{Th}_{\text{MR2}}=4$ ppb $^{149}\text{Sm}_{\text{MR2}}=4$ ppb $^{42}\text{Ca}_{\text{MR2}}=1$ ppm	60 ml	600 μL $^{42}\text{Ca}_{\text{MR1}}$ (1000 ppm) + 250 μL $^{235}\text{U}_{\text{MR}}$ (1 ppm) + 2.4 ml $^{230}\text{Th}_{\text{MR1}}$ (100 ppb) + 0.034 μL $^{149}\text{Sm}_{\text{MR}}$ (7 ppm) + 56.766 mL HNO_3 5N
Spiked solutions for spikes calibration			
S: concentrated standard solutions used for spike	$^{238}\text{U}_{\text{S}}$	125 ml	^{238}U tailored solution HNO_3 5N 1015ppm
	$^{232}\text{Th}_{\text{S}}$		^{232}Th tailored solution HNO_3 5N 993 ppm



calibration	Sm _S natural Ca _S natural		Sm natural solution HNO ₃ 5N 1006 ppm (¹⁴⁷ Sm =14.99%; ¹⁴⁹ Sm = 13.82%) Ca natural solution HNO ₃ 5N 1003 ppm (⁴⁰ Ca=96.94%, ⁴² Ca=0.65%, ⁴³ Ca=0.14%)
U_s(III) : freshly made multi-step dilutions to obtain 4 ppb ²³⁸ U mono-elemental standard solution	²³⁸ U _S (I) ²³⁸ U _S (II) ²³⁸ U _S (III)	8 ml ml 8ml	I) 10 ppm ²³⁸ U=80 μL ²³⁸ U 1015ppm +7.92 ml HNO ₃ 5N II) 100 ppb ²³⁸ U=10 μL ²³⁸ U 80 ppm +7.92 ml HNO ₃ 5N III) 4 ppb ²³⁸ U=320 μL ²³⁸ U 100 ppb + 7.68 ml HNO ₃ 5N
Th_s(III) : freshly made multi-step dilutions to obtain 4 ppb ²³² Th mono-elemental standard solution	²³² Th _S (I) ²³² Th _S (II) ²³² Th _S (III)	8 ml ml 8ml	I) 10 ppm ²³² Th = 80 μL ²³² Th 993ppm +7.920 ml HNO ₃ 5N II) 100 ppb ²³² Th = 80 μL ²³² Th 10 ppm +7.920 ml HNO ₃ 5N III) 4 ppb ²³² Th = 320 μL ²³² Th 100 ppb + 7.680 ml HNO ₃ 5N
Sm_s(III) : freshly made multi-step dilutions to obtain 4 ppb ¹⁴⁹ Sm mono-elemental standard solution	¹⁴⁹ Sm _S (I) ¹⁴⁹ Sm _S (II) ¹⁴⁹ Sm _S (III)	10 ml 1l 8 ml	I) 1 ppm Sm nat = 10 μL Sm nat + 9.990 ml HNO ₃ 5N II) 70 ppb Sm nat = 0.7 ml Sm nat 1 ppm + 9.3 ml HNO ₃ 5N III) 4 ppb Sm nat = 0.460 ml Sm nat 70 ppb + 7.54 ml HNO ₃ 5N
SS : freshly spiked standard solutions prepared using MR2	U _{SS}	2 ml	50 μL ²³⁸ U _S (III) (4 ppb) + 50 μL ²³⁵ U _{MR2} (4 ppb) + 1.900 ml HNO ₃ 1N



and S solutions	Th _{SS}	50 μL ²³² Th _S (III) (4 ppb) + 50 μL ²³⁰ Th _{MR2} (4 ppb) + 1.9 ml HNO ₃ 1N
	Sm _{SS}	50 μL ¹⁴⁹ Sm _S (III) (4ppb) + 50 μL ¹⁴⁹ Sm _{MR2} (4ppb) + 1.9 ml HNO ₃ 1N
	Ca _{SS}	5 μL Ca _S (1000 ppm) + 50 μL ⁴² Ca _{MR2} (1 ppm) + 1.945 ml HNO ₃ 1N

250 2.5 U, Th (Sm and Ca) analysis by ICP-MS

The solutions obtained by chemical dissolution of the samples are then analyzed with an ICP-MS in order to determine the U, Th and Sm (Ca for apatite) signal intensities. We now mainly use a High Resolution Inductively Coupled Plasma Mass Spectrometer –HR-ICP-MS - ELEMENT XR from Thermo Scientific) at GEOPS laboratory since 2016, that allows the U, Th and Sm isotopes to be measured at low resolution (300) while Ca is measured at high resolution (10 000). In addition, we also use a quadrupole ICP-QMS seriesII CCT Thermo-Electron at LSCE (Gif/Yvette; France) and an Agilent 7900 quadrupole ICP-MS at IPGP (France) in order to measure the U, Th and Sm contents.

The U, Th, Sm and Ca abundances are then deduced from the measured ²³⁵U/²³⁸U, ²³⁰Th/²³²Th, ¹⁴⁹Sm/¹⁴⁷Sm and ⁴²Ca/⁴³Ca ratios and the following equations derived from Evans et al. (2005) with a homemade Excel WorkBook based on VBA automatization software.

$$260 \quad {}^{238}\text{U} = \left(m_{spk} (g) \times [{}^{235}\text{U}_{spk}] \times 10^{-9} \right) \times \frac{1}{\left(\left(\frac{{}^{235}\text{U}}{{}^{238}\text{U}} \right)_{spk} \right)} \times \frac{\left(\left(\frac{{}^{235}\text{U}}{{}^{238}\text{U}} \right)_{sp} - \left(\frac{{}^{235}\text{U}}{{}^{238}\text{U}} \right)_{BSP} \right)}{\left(\left(\frac{{}^{235}\text{U}}{{}^{238}\text{U}} \right)_{Nat} - \left(\frac{{}^{235}\text{U}}{{}^{238}\text{U}} \right)_{sp} \right)} \quad (4)$$

$${}^{232}\text{Th} = \left(m_{spk} (g) \times [{}^{230}\text{Th}_{spk}] \times 10^{-9} \right) \times \frac{1}{\left(\left(\frac{{}^{230}\text{Th}}{{}^{232}\text{Th}} \right)_{spk} \right)} \times \frac{\left(\left(\frac{{}^{230}\text{Th}}{{}^{232}\text{Th}} \right)_{BSP} - \left(\frac{{}^{230}\text{Th}}{{}^{232}\text{Th}} \right)_{sp} \right)}{\left(\left(\frac{{}^{230}\text{Th}}{{}^{232}\text{Th}} \right)_{sp} \right)} \quad (5)$$



$$^{147}\text{Sm} = \left(m_{\text{spk}} (\text{g}) \times \left[^{149}\text{Sm}_{\text{spk}} \right] \times 10^{-9} \right) \times \frac{1}{\left(\left(\frac{^{149}\text{Sm}}{^{147}\text{Sm}} \right)_{\text{spk}} \right)} \times \frac{\left(\left(\frac{^{149}\text{Sm}}{^{147}\text{Sm}} \right)_{\text{sp}} - \left(\frac{^{149}\text{Sm}}{^{147}\text{Sm}} \right)_{\text{BSP}} \right)}{\left(\left(\frac{^{149}\text{Sm}}{^{147}\text{Sm}} \right)_{\text{Nat}} - \left(\frac{^{149}\text{Sm}}{^{147}\text{Sm}} \right)_{\text{sp}} \right)} \quad (6)$$

$$^{43}\text{Ca} = \left(m_{\text{spk}} (\text{g}) \times \left[^{42}\text{Ca}_{\text{spk}} \right] \times 10^{-9} \right) \times \frac{1}{\left(\left(\frac{^{42}\text{Ca}}{^{43}\text{Ca}} \right)_{\text{spk}} \right)} \times \frac{\left(\left(\frac{^{42}\text{Ca}}{^{43}\text{Ca}} \right)_{\text{sp}} - \left(\frac{^{42}\text{Ca}}{^{43}\text{Ca}} \right)_{\text{BSP}} \right)}{\left(\left(\frac{^{42}\text{Ca}}{^{43}\text{Ca}} \right)_{\text{Nat}} - \left(\frac{^{42}\text{Ca}}{^{43}\text{Ca}} \right)_{\text{sp}} \right)} \quad (7)$$

with spk (spike), sp (sample), BSP (spiked blank), Nat (natural ratio: $^{235}\text{U}/^{238}\text{U} = 0.00725$; $^{149}\text{Sm}/^{147}\text{Sm} = 0.9$ ($^{147}\text{Sm} = 14.99\%$ and $^{149}\text{Sm} = 13.8\%$) and $^{42}\text{Ca}/^{43}\text{Ca} = 4.8$ ($^{42}\text{Ca} = 0.647\%$ and $^{43}\text{Ca} = 0.135\%$). We obtain abundances in nanogram (10^{-9} g) and spike concentrations in ppb. In addition, the same equations can be reversed to determine the concentration of the spike isotopes ^{235}U , ^{230}Th , ^{149}Sm and ^{42}Ca .

We obtain the weight of the apatite grain(s) from the measurement of ^{43}Ca , for which we use the composition of a pure fluoro-apatite ($\text{Ca}_5(\text{PO}_4)_3\text{F}$) containing 40 wt. % Ca in one apatite crystal. Thus, the apatite weight is given by equation (8):

$$\text{weight}(\mu\text{g}) = \frac{^{43}\text{Ca} \times 10^{-9}}{0.135/100} \times \frac{1}{0.4 \times 10^{-6}} \quad (8)$$

The factor 0.135 refers to the natural isotope abundance of the ^{43}Ca isotope.

The measurement of the Ca content and the deduced apatite crystal weight combined to the measurements of U, Th, Sm abundances then allow the U, Th and Sm concentrations of the Durango fragments to be determined. Determination of crystal weight is also useful to ensure that the criteria imposed for grain selection, i.e. (i) crystal size ($L, W, T > 60 \mu\text{m}$), (ii) geometry (well-shaped prisms), and (iii) purity (inclusion-free crystals) have been respected. Guenther et al. (2016) have already performed a complete work on determining apatite and zircon weights by measuring the Ca and Zr contents.

2.6 (U-Th)/He age reduction

The (U-Th)/He age (in Ma) is calculated assuming a linear production of ^4He with time, using the determined U, Th and Sm concentrations such as:



$$280 \quad \frac{(U-Th)}{He} age(Ma) = \frac{4He}{P^* \times 10^{-6}} \quad (9)$$

where P^* is the instantaneous production of 4He , i.e. the 4He concentration produced in one year in ccSTP/g, and 4He is the measured 4He concentration in ccSTP/g. P^* is calculated using the following equation:

$$285 \quad P^* \left(\frac{8 \times [^{238}U] \times 10^9}{238 \times 0.69} \times \lambda_{238U} + \frac{7 \times [^{238}U] \times 10^9}{235 \times 137.88 \times 0.69} \times \lambda_{235U} + \frac{6 \times [^{232}Th] \times 10^9}{232 \times 0.69} \times \lambda_{232Th} + \frac{[^{147}Sm] \times 10^9}{147 \times 0.69} \times \lambda_{147Sm} \right) \times 22414 \quad (10)$$

With $\lambda_{238U}(y^{-1}) = Ln(2)/(4.47 \times 10^9)$; $\lambda_{235U}(y^{-1}) = Ln(2)/(7.04 \times 10^8)$; $\lambda_{232Th}(y^{-1}) = Ln(2)/(1.40 \times 10^{10})$; $\lambda_{147Sm}(y^{-1}) = Ln(2)/(1.06 \times 10^{11})$, and with $[^{238}U]$, $[^{232}Th]$ and $[^{147}Sm]$ the measured concentrations in ppb. The value of 137.88 is the $^{238}U/^{235}U$ natural isotopic ratio, and 1 mol occupies 22414 cc at standard pressure and temperature conditions (ccSTP). The assumption that the 4He production is linear is valid for ages lower than ~ 150 Ma, as the half-life of the U, Th and Sm are important compared to 150 Ma.

For an ICP-MS session, the (U-Th)/He data reduction Excel WorkBook is able to calculate the U-Th-Sm contents and their associated standard deviations for the different minerals analyzed, according to the chemical dissolution protocol followed. The Excel WorkBook also calculates the (U-Th)/He data, which include U, Th, Sm contents and the effective uranium content (eU) both in ppm, the Th/U and Sm/Th ratios and the (U-Th)/He age.

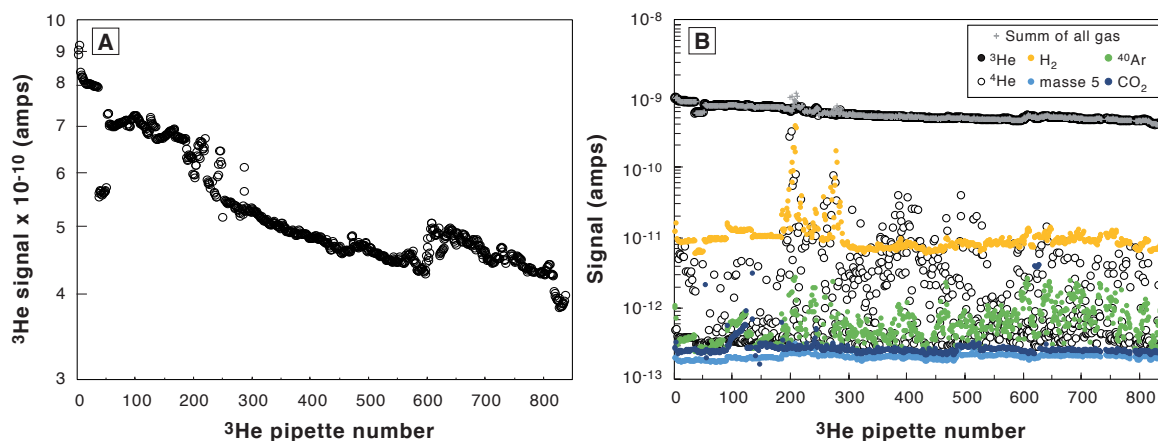
295 3 (U-Th)/He results and discussion

3.1 Helium quadrupole analysis

One aspect of quadrupole mass spectrometry is the variable response in terms of ionization and signal analysis of such instruments. This behavior has also been observed on the quadrupole adopted here for analyses of rare gases and is illustrated on Figure 3A. The signal of the 3He spike is reported as a function of the number of the pipettes extracted, over a period of 5 months of analysis. The 3He signal fluctuates significantly although the 3He amount in each pipette should decrease smoothly following a law that depends on the volume of the cylinder and the pipette volume (here ~ 4000 and ~ 0.5 cc, respectively; see equation (1)). The advantage of using a 3He spike for isotopic dilution is to thwart the impact of the nonlinear answer of the

quadrupole mass spectrometer with time (Farley, 2002; House et al., 2000), but it also allows the total gas pressure to be buffered in the mass spectrometer if the introduced ^3He signal is large enough compared to the other signals.

305 Figure 3B presents the various signals measured with the quadrupole mass spectrometer (H_2 , ^3He , ^4He , ^{40}Ar , CO_2 , and masse 5 that represents the background noise) during the same 5 months of analysis (~10 to 30 analyses per days, 5 days a week). The ^3He clearly controls the total pressure inside the mass spectrometer during the analysis, independently from the pressure of ^4He gas released from the sample. The use of spike rich in ^3He allows to get a stable and uniform total pressure in the mass spectrometer, for any degassed sample analyzed.



310

Figure 3: Evolution of the measured ^3He signal with the pipette number (from January to June 2019). (A) Decrease of the spike ^3He signal. (B) Evolution of all the measured signals (^3He black dots; ^4He : open black dots; H_2 : orange dots; masse 5 (background noise): light blue dots; ^{40}Ar : green dots and CO_2 : dark blue dots; crosses: summation of all the signals).

315

However, the quadrupole signals are variable and sometimes erratic within few percent of the signal over weeks to months periods of time (Fig. 3A). To correct for the quadrupole drift, we introduce a correcting factor, noted D in the calculation of the ^3He , pipette content (equation 1). This parameter acts by modifying the value of the pipette volume, V2 in equation (1), to counterbalance the variations of the quadrupole sensitivity. Figures 4C and D presents the Durango apatite (U-Th)/He ages obtained from measurements over a period of two months using two coupled values of the drift parameter D and ^3He , calibrated
320 content. One can observe that the (U-Th)/He ages obtained for the Durango apatite remain constant and are more reproducible using a D value of 99.937×10^{-2} as compared to 99.987×10^{-2} . In the present case, it just depletes the tank in ^3He more quickly.

This operation is done for every batch of (U-Th)/He analysis that corresponds to mostly to 1 to 2 months of He analysis. Each couple of values of the $^3\text{He}_c$ and D parameters are recorded allowing to detect any problem during the measurements. Most of the time, the sensibility is not evolving and the same D and $^3\text{He}_c$ values are used. However, each time the filament or the voltage of the multiplier are changed, those values needed to be tuned. This way determining the mass spectrometer sensitivity makes precise knowledge of the volumes of the pipette system (V1 and V2) not so important.

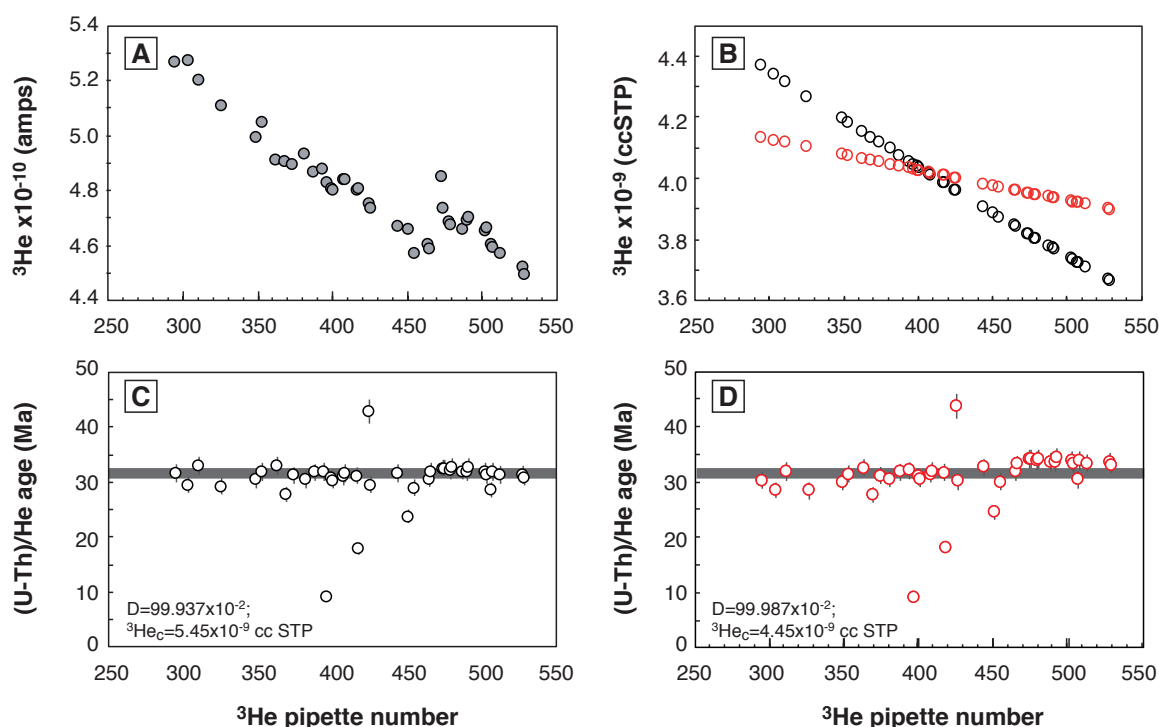


Figure 4: Evolution of the Durango apatite age as a function of the pipette number. (A) Evolution of the ^3He signal over the period of analysis. (B) Evolution of the calculated ^3He content of each pipette for two different drift value D (black dots or red dots) and $^3\text{He}_c$ calibrated content, using equation (1). (C) and (D) calculated Durango AHe ages for the different D drift value and $^3\text{He}_c$ calibrated content.

In addition to the ^3He pipette number associated to each measurement, we use a specific code name. As an example, for the Durango apatite, the code name D19P11A can be read as Durango, year 2019, planchette n°11, aliquot A. This designation using the name of sample and its analysis date allows to better organize the He analyses database and data backup from a chronological point of view.

3.2 Helium magnetic sector analysis

In comparison to quadrupole mass spectrometers, magnetic sector mass spectrometers have a more stable and linear response of ionization and thus allow for a better analysis. To test the response of the modified VG5400 mass spectrometer and better calibrate the ^4He cylinder, we performed multiple analyzes of fragments of Durango apatites having different sizes (dozens to hundreds of micrometers long fragments). After degassing, the U, Th and Sm contents of the fragments are determined and, assuming an age of 31.02 ± 1.01 (McDowell et al., 2005), the amount of ^4He for each fragment is calculated. This operation was performed twice at different times, using the VG5400 tuned with different source parameters and using different He line conditions, one with the use of a cryogenic trap allowing to concentrate the gas in a smaller volume, the other without. Using the correlation between the calculated ^4He in ccSTP and the ^4He signal in count per second (cps), the sensitivity was determined (Fig. 5).

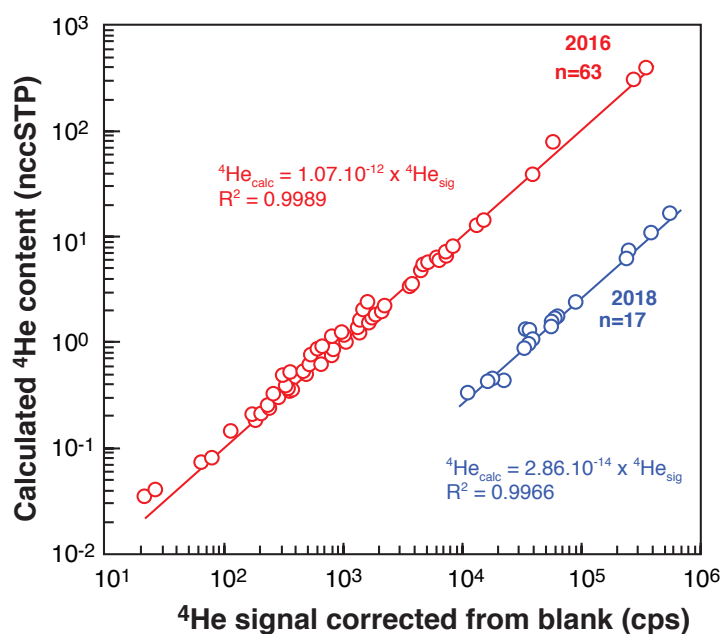


Figure 5: VG5400 magnetic sector mass spectrometer sensitivity determined using fragments of Durango apatite. In 2016, a He sensitivity of 1.1×10^{-12} ccSTP He/cps was obtained. In 2018, the addition of a cryogenic trap and modifications of source parameters allowed to get a better sensitivity of 2.9×10^{-14} ccSTP He/cps (cps: counts per second). n is the number of analyzed fragments.



For the two different conditions, the measured ^4He signal and the ^4He content calculated from measured U-Th-Sm display a very good linear correlation ($r^2 > 0.99$, Fig. 5). Sensitivity values of 1.1×10^{-12} ccSTP He/cps and 2.9×10^{-14} ccSTP He/cps were thus determined, additionally showing that the use of the cryogenic trap increases the sensitivity by a factor ~ 40 . Such analyzes of Durango apatite fragments are therefore useful to test the electron multiplier and counting system responses, which turned out to be linear from thousands to hundreds of thousands of cps for He, without any impact of the dead counting time. The use of both a ^4He cylinder and the Durango apatite fragments is thus important to follow the evolution of the filament and analyzer conditions through time.

360 3.3 U, Th, Sm chemistry and blanks

Acid blanks are regularly analyzed and allow the acid quality to be controlled. Low intensities are measured for ^{235}U and ^{230}Th , i.e. < 20 cps, meanwhile the intensities for ^{238}U and ^{232}Th are hundred times higher. Higher signal intensities for all the isotopes are measured in Blk-ch, indicating that the chemical dissolution method adds some contamination to the sample solutions. Such contribution is nevertheless very negligible compared to the intensities of the signals observed for the apatite and zircon samples (100 000 cps).

For apatite, U, Th and Sm in blanks are low in comparison with the U, Th, Sm contents of the apatite, as already stated by Reiners and Nicolescu (2007). Figure 6 presents the evolution of the measured $^{235}\text{U}/^{238}\text{U}$, $^{230}\text{Th}/^{232}\text{Th}$ and $^{149}\text{Sm}/^{147}\text{Sm}$ isotopic ratios for spiked blank (BSP), spiked blank chemistry (BSP-ch) and for Durango apatite sample (Sp) solutions. For a spiked sample (Sp), the $^{235}\text{U}/^{238}\text{U}$, $^{230}\text{Th}/^{232}\text{Th}$ and $^{149}\text{Sm}/^{147}\text{Sm}$ ratios range between the BSP-ch value and the natural value (i.e. $^{235}\text{U}/^{238}\text{U} = 0.00725$; $^{230}\text{Th}/^{232}\text{Th} = 0$ (no natural ^{230}Th atoms) and $^{149}\text{Sm}/^{147}\text{Sm} = 0.9$), as can be observed in Figure 6. The isotopic ratio values for the BSP and BSP-ch blanks do not vary by more than few percent through the different analyzes and are orders of magnitude higher than for the sample (Sp). The BSP-ch display lower $^{235}\text{U}/^{238}\text{U}$, $^{230}\text{Th}/^{232}\text{Th}$ and $^{149}\text{Sm}/^{147}\text{Sm}$ values compared to the BSP (Fig. 6), showing that the chemistry protocol has an impact on the U, Th and Sm isotopes in solution. However, this effect remains insignificant compared to the Durango apatite U, Th, Sm contents, and does not influence the (U-Th)/He age. Nevertheless, blanks are always well characterized, as for natural apatite crystals, the U, Th and Sm contents are usually lower than for Durango.

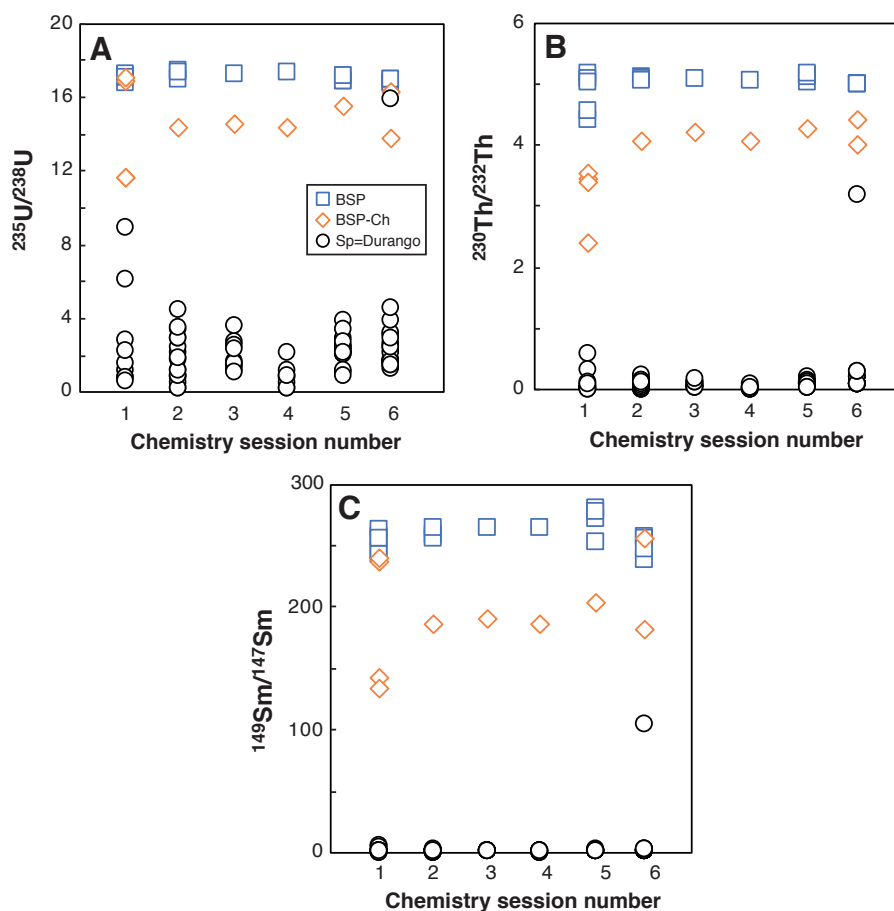


Figure 6: Evolution of the $^{235}\text{U}/^{238}\text{U}$, $^{230}\text{Th}/^{232}\text{Th}$ and $^{149}\text{Sm}/^{147}\text{Sm}$ ratios obtained for BSP, BSP-ch and Durango apatite Sp solutions, for 6 different chemistry session.

380

In opposition to apatite, the chemical dissolution for zircon requires the acquisition and maintenance of more complex laboratory material, such as PFA vials and a high temperature/high pressure Parr bomb and concentrated acids like HF. Tests carried out on all types of blanks BSP, BSP-ch and BSPch-Nb have been done over 18 series of sample analyzes performed between March 2016 and February 2018. Under constant vessel cleaning protocol and acid quality conditions, comparison of the analyzed U and Th isotopes are presented in Figure 7. Isotopic ratios measured in BSP-ch ($^{235}\text{U}/^{238}\text{U}=16.1\pm 0.3$; $^{230}\text{Th}/^{232}\text{Th}=4.8\pm 0.5$) showed a slight reduction of their values compared to those found in BSP ($^{235}\text{U}/^{238}\text{U}=17.3\pm 1.0$; $^{230}\text{Th}/^{232}\text{Th}=5.1\pm 0.2$), indicating again a small contamination during the chemical protocol (Fig. 7). The loss of elements and



more specifically of Th when HF+HNO₃ acids are used has already been well described (e.g. Révillon and Hureau-Mazaudier, 2009; Yokoyama et al., 1999), and the effect can be seen on Figure 7, where the ²³⁵U/²³⁸U and ²³⁰Th/²³²Th ratios are lower than
390 for the BSP. In addition, the use of Nb capsules (BSP-ch-Nb) also impacts the U and Th budgets and leads to a massive reduction of the ratios (maxima ²³⁵U/²³⁸U=16.2±1.0; ²³⁰Th/²³²Th=4.1±0.9 and recorded minima down to ²³⁵U/²³⁸U=12.0; ²³⁰Th/²³²Th=1.7; Fig. 7).

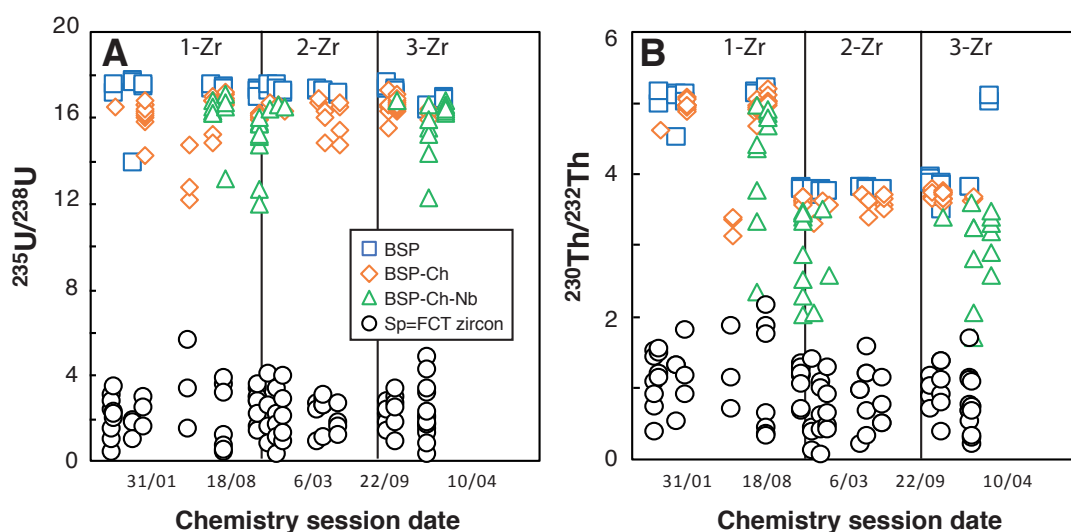


Figure 7: Evolution of the ²³⁵U/²³⁸U and ²³⁰Th/²³²Th ratios obtained for BSP, BSP-ch, BSP-ch-Nb and FCT zircon solutions for
395 different chemistry session. 1-Zr, 2-Zr and 3-Zr refer to the spike solution names used during the dissolution.

The impact of the niobium capsule on U and Th signals has already been noted by Reiners and Nicolescu (2007), and reported to be more significant for the Th content. The differences in ²³⁵U/²³⁸U and ²³⁰Th/²³²Th ratios between the different blanks (BSP, BSP-ch, BSP-Ch-Nb) are associated with some isotope fractionation, with a calculated decrease of respectively
400 4 to 6% for the ²³⁵U/²³⁸U ratio and 10 to 20% for the ²³⁰Th/²³²Th ratio, compared to the expected ratios given by the spiked solutions without Nb. The shift for these ratios is systematic but variable from one solution to another, particularly for the ²³⁰Th/²³²Th ratio, showing values down to 60% of the expected spiked solution ratio. A correction of the impact of the niobium capsule on the U and Th solution needs to be considered as this effect can result in a shift of the zircon (U-Th)/He ages up to ~20%.



405 3.4 Durango apatite and FCT zircon (U-Th)/He age reproducibility

The Durango apatite is constantly analyzed in the laboratory to check for the He mass spectrometer sensitivity evolution though time as well as the evolution of (U-Th)/He age and U, Th and Sm contents. As the dissolution protocol for apatite has a very low impact on the U, Th and Sm content determination by ICP-MS analysis, the measurement of Durango apatite acts as a sensor and regularly allows to detect any analytical problem. As an example, Figure 8 presents the values of the (U-Th)/He
410 ages, and Th/U and Sm/Th ratios acquired from March to December 2019 by both the He and VG lines, and values are reported in Table S1. The mean of the (U-Th)/He age is 31.1 ± 1.4 Ma in agreement with the age of 31.02 ± 1.01 Ma from McDowell et al. (2005).

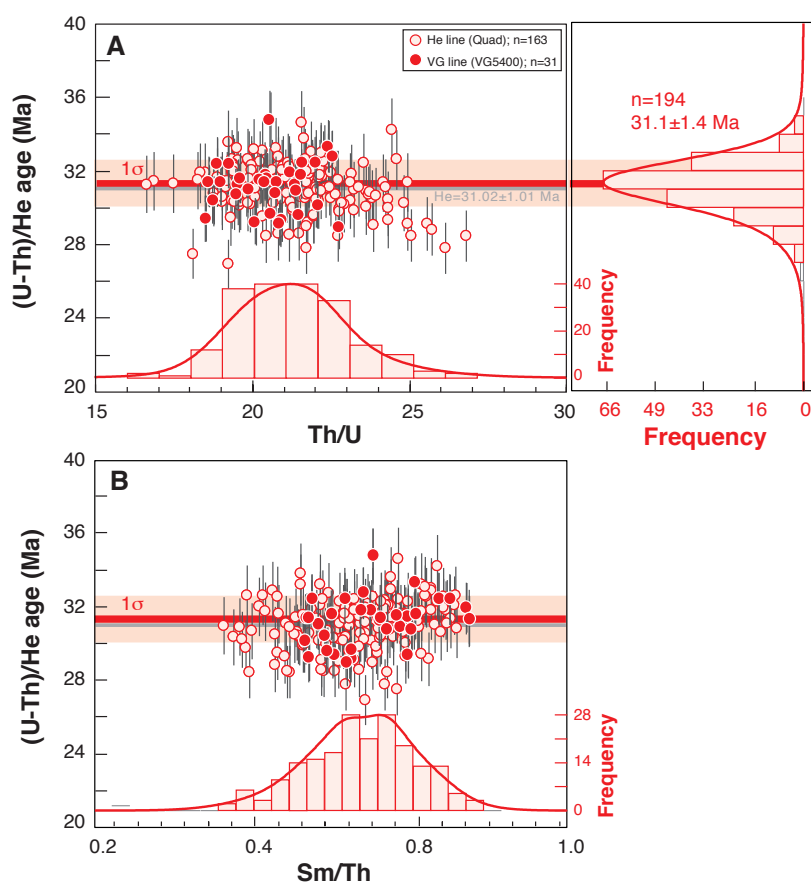
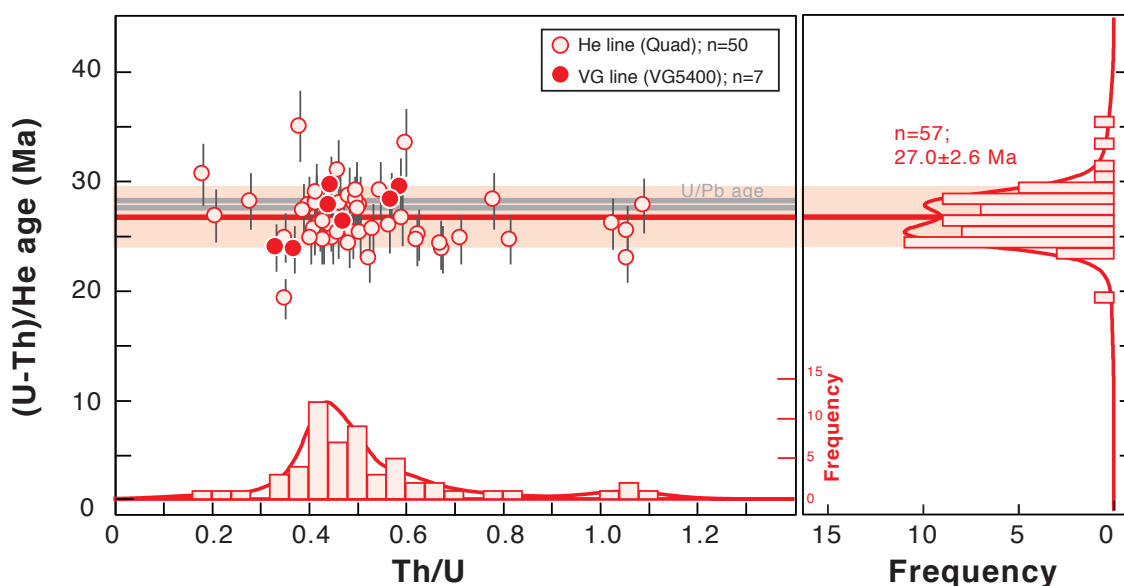


Figure 8: Durango (U-Th)/He age dispersion (at 1σ) as a function of Th/U (A) or Sm/Th ratios (B). Durango AHe ages and
415 elemental ratios acquired from March to December 2019 using the He line (open red circles) or the VG line (red circles).

Histogram representation of the He ages, Th/U and Sm/Th ratios has been constructed using Radial Plotter (Vermeesch, 2009).

A typical mean error of <5% (1σ) is obtained on each AHe age by using either quadrupole or magnetic sector mass spectrometers, without any evident difference over a large period of time. This error can be interpreted as the quadratic sum of the errors on the coupled analyzes of the U-Th-Sm and the He contents and are associated with the calibration. Our (U-Th/He) ages on unknown apatite compare well within error with other laboratories data (e.g Ketcham et al., 2018). In addition, our strategy developed to determine the Ca concentration allows us to obtain the weight of the Durango fragment(s) and thus to calculate the U, Th, Sm concentrations in ppm (Table S1). Mean values of U=19±4 ppm, Th=412±68 ppm and Sm=38±7 ppm have been obtained and the U content is similar to that obtained by Schneider et al. (2015) and Yanga et al. (2014).

Fish Canyon Tuff zircon crystals have been analyzed at the GEOPS laboratory as standards for the ZHe method. The U and Th losses during dissolution, due to the niobium impact, are corrected for the determination of the U and Th concentrations in zircons. (U-Th)/He ages were obtained on 57 crystals of FCT zircons analyzed using the He and VG lines and are reported in Figure 9 as a function of the Th/U ratio, and in Table S2.



430 **Figure 9:** FCT zircon (U-Th)/He age dispersion as a function of the Th/U ratio, for the data obtained in 2018 using the He and VG lines. Histogram representation of the (U-Th)/He age and Th/U ratio values have been constructed using Radial Plotter (Vermeesch, 2009). An U/Pb age of 28.5 ± 0.06 Ma has been published by Schmitz and Bowring (2001).



We obtained a mean age of 27.0 ± 2.6 Ma (1σ) and a mean Th/U ratio of 0.4 on zircon crystal from C.W. Naeser
435 collection (K/Ar age of 27.9 ± 0.7 Ma; Naeser et al., 1991) (Fig. 9). The standard dispersion of the ZHe ages is $\sim 9\%$ and is
comparable to the natural dispersion observed in the ZHe values given in the literature (e.g. Ault et al., 2018; Guenther et al.,
2014; Reiners, 2005). The Th/U dispersion of 37% also corresponds to the natural dispersion observed in the Th/U ratio of the
Fish Canyon zircon standard (e.g. Reiners et al., 2002). The (U-Th)/He age results are comparable with (U-Th)/He literature
440 data that range from 27.3 ± 1.0 to 29.8 ± 2.7 Ma (Dobson et al., 2008; Gleadow et al., 2015; Reiners et al., 2002; Tagami et al.,
2003; Tibari et al., 2016). Th/U ratios vary between 0.42 ± 0.15 Ma (Tagami et al., 2003) and 0.63 ± 0.14 Ma (Tibari et al., 2016)
in the literature. The mean (U-Th)/He age obtained in this study is slightly younger by 5% than the U/Pb age of 28.5 ± 0.06 Ma
obtained by Schmitz and Bowring (2001), but still in good agreement within error bars (Fig. 9). The slight ZHe age difference
could also be explained by the measured variable ages of the Fish Canyon Tuff zircon as a function of the sampling site
(Gleadow et al., 2015). An second option is that since similar ages are obtained by degassing either on the He or VG line, that
445 the slight shift in the (U-Th)/He age may be associated with the He content determination for few percent, but also associated
to the U and Th content determination and finally to the impact of the niobium precipitation during zircon dissolution. The
loss of U and more specifically of Th associated to the use of HF+HNO₃ (Révillon and Hureau-Mazaudier, 2009; Yokoyama
et al., 1999), and from the use of Nb capsule (Reiners and Nicolescu, 2007) have already been taken into account on the blank
correction. However, the slight lower ZHe ages obtain in this study could also be associated with an under correction of the
450 impact of the zirconium brought into solution that could cause a slight loss in Th that is not taken into account in the blank
correction. To estimate such an impact, additional work should be carried out to fully understand the U and Th isotope
fractionation during this chemical protocol.

4 Conclusion

This contribution presents the (U-Th)/He analysis protocols developed for over more than ten years and shares all the
455 empirical and analytical aspects observed during the different steps of the protocol: sample preparation, mineral hand picking,
He analysis, dissolution and U, Th and Sm content determination. In the light of our experience, we propose:



- a simple method to determine the temperature of the heated metallic (Pt and Nb) capsules that contain the apatite or zircon crystals during laser firing in the range 900-1200°C (visible light emission wavelength);
- a method to calibrate He sensitivity using quadrupole and magnetic sector mass spectrometers;
- 460 - the protocols to dissolve apatite and zircon crystals and to clean laboratory vessels after chemical digestion;
- the protocol to calibrate the U, Th and Sm spikes;
- the method used to track the U, Th and Sm blank evolution and determine U, Th and Sm contents;

We adopted the Durango apatite as a standard to perform the He calibration and check for He, U-Th-Sm analytical problems and are able to determine (U-Th)/He ages with an error of less than 5%. Our choice is also related to the fact that Durango is an easy-to-use mineral due to its high purity, its rapid dissolution protocol and the strong reproducibility during analyses. For the long-term quality control of the (U-Th)/He data, attention needs to be paid to evaluate precisely the drift of blanks through time and those of the (U-Th)/He ages and Th/U ratios (with Sm/Th when possible) obtained on standards (Durango apatite and Fish Canyon Tuff zircon).

470 **Author contribution:** CG, RP, PS, LT, JM and DB designed the experiments, CG, RP, FA, AD, CS, FH, GM, GD participated in the data acquisition. LT developed the Monte Carlo simulation QTLFT software and AD the Excel WorkBook automatization software. CG prepared the manuscript with contributions from all co-authors.

Competing interests: The authors declare that they have no conflict of interest.

475 **Acknowledgments**

The analytical work and the He and VG lines building have been funded thanks to INSU-Relief, FORPRO and Tellus programs, INSU mi-lourd, Division de la recherche of the Paris Sud University, ERM Paris Sud program, ANR-06-JCJC-0079 and ANR-12-NS06-0005-01 HeDiff projects. M. Pagel is warmly thanked for his help in funding the cryogenic trap. IUT mesure physique internships trainees P. Marty, S. Lemaire, E. Cornier, M. Di Giacomo, G. Ya, P. Boutteville, M. Form, N. Etienne, 480 C. Morelière, H. Vicente and B. Canguilhem are warmly thanked for their work and implication in LabView programming of



the different parts of the He and VG lines. We thanked P. Reiners and U. Chowdhury for sharing their knowledge on zircon dissolution protocols and J. R. Metcalf for the location of the FCT outcrop and advices. We warmly thanked PC Hackspacher for the donation of gem quality Durango apatite crystals and C.W. Naeser for the donation of Fish Canyon Tuff zircon fraction. M. Moreira is thanked for his help on building the valves controlling electronics and help on the building of the VG line. J.L. Birck is thanked for the loan of the external filament extinction pyrometer. P. Burckel, E. Douville and L. Bordier are thanked for the U-Th-Sm analyses at IPGP and LSCE.

References

- Allard, T., Gautheron, C., Bressan-Riffel, S., Balan, E., Selo, M., Fernandes, B.S., Pinna-Jamme, R., Derycke, A., Morin, G., Taitson Bueno, G. and Do Nascimento, N.R., Combined dating of goethites and kaolinites from ferruginous duricrusts. *Chem. Geol.* 479, 136-150. <https://doi.org/10.1016/j.chemgeo.2018.01.004>, 2018.
- Ault, A.K., Guenther, W.R., Moser, A.C., Miller, G.H., and Refsnyder, K.A., Zircon selection reveals (de)coupled zircon metamictization, radiation damage, and He diffusivity. *Chem. Geol.*, <https://doi.org/10.1029/2018TC005312490>: 1-12, 2018.
- Burnard, P.G., and Farley, K.A., Calibration of pressure-dependent sensitivity and discrimination in Nier-type noble gas ion sources. *Geochem., Geophys. Geosy.*, 1: 2000GC000038, 2000.
- Cros, A., Gautheron, C., Pagel, M., Berthet, P., Tassan-Got, L., Douville, E., Pinna-Jamme, R. and Sarda, P., 4He behavior in calcite filling viewed by (U-Th)/He dating, 4He diffusion and crystallographic studies. *Geochim. Cosmochim. Acta*, 125: 414-432, <http://dx.doi.org/10.1016/j.gca.2013.09.038>, 2014.
- Dobson, K.J., Stuart, F.M., and Dempster, T.J., U and Th zonation in Fish Canyon Tuff zircons: Implications for a zircon (U-Th)/He standard. *Geochim. Cosmochim. Acta*, 72(19): 4745-4755, doi:10.1016/j.gca.2008.07.015, 2008.
- Evans, N.J., Byrne, J.P., Keegan, J.T., and Dotter, L.E., Determination of uranium and thorium in zircon, apatite, and fluorite: Application to laser (U-Th)/He thermochronology. *J. Ana. Chem.*, 60(12): 1300-1307, 2005.
- Farley, K.A., Helium diffusion from apatite: general behavior as illustrated by Durango fluorapatite, *J. Geophys. Res.*, 105: 2903-2914, 2000.
- Farley, K.A., (U-Th)/He dating: Techniques, calibrations, and applications. In: *geochemistry, R.i.m. (Ed.), Noble Gases in Geochemistry and Cosmochemistry*, pp. 819-844, DOI:10.2138/rmg.2002.47.18, 2002.
- Foeken, J.P.T., Stuart, F.M., Dobson, K.J., Persano, C., and Vilbert, D., A diode laser system for heating minerals for (U-Th)/He chronometry. *Geochem Geophys*, 7(4): 1-9, <https://doi.org/10.1029/2005GC001190>, 2006.
- Gautheron, C., Tassan-Got, L., A Monte Carlo approach of diffusion applied to noble gas/ helium thermochronology. *Chem. Geol.*, 273: 212-224, doi:10.1016/j.chemgeo.2010.02.023, 2010.



- Gautheron, C., Tassan-Got, L., Ketcham, R.A., and Dobson, K.J., Accounting for long alpha-particle stopping distances in (U-Th-Sm)/He geochronology: 3D modeling of diffusion, zoning, implantation, and abrasion. *Geochim. Cosmochim. Acta*, 96: 44-56, <http://dx.doi.org/10.1016/j.gca.2012.08.016>, 2012.
- Gautheron, C., Zeitler, P.K., Noble Gases Deliver Cool Dates from Hot Rocks. *Elements*, 16: 303-309, DOI: 10.2138/gselements.16.5.303, 2020.
- 515
- Gleadow, A., Harrison, M., Kohn, B.P., Lugo-Zazuta, R., and Phillips, D., The Fish Canyon Tuff: A new look at an old low-temperature thermochronology standard. *Earth Planet. Sci. Lett.*, 424: 95-108, <https://doi.org/10.1016/j.epsl.2015.05.003>, 2015.
- Guenther, W.R., Reiners, P.W., and Chowdhury, U., Isotope dilution analysis of Ca and Zr in apatite and zircon (U-Th)/He chronometry. *Geochem Geophys*, 17: 1623-1640, DOI 10.2475/03.2013.01, 2016.
- 520
- Guenther, W.R., Reiners, P.W., DeCelles, P.G., and Kendall, J., 2014. Sevier belt exhumation in central Utah constrained from complex zircon (U-Th)/He data sets: Radiation damage and He inheritance effects on partially reset detrital zircons. *GSA Bulletin*, B31032: 1, <https://doi.org/10.1130/B31032.1>, 2014.
- House, M.A., Farley, K.A., and Stockli, D., Helium chronometry of apatite and titanite Nd-YAG laser heating. *Earth Planet. Sci. Lett.*, 183: 365-368, 2000.
- 525
- Ketcham, R.A., Gautheron, C., and Tassan-Got, L., Accounting for long alpha-particle stopping distances in (U-Th-Sm)/He geochronology: refinement of the baseline case. *Geochim. Cosmochim. Acta*, 75: 7779-7791, doi:10.1016/j.gca.2011.10.011, 2011.
- Ketcham, R.A., van der Beek, P., Barbarand, J., Bernet, M. and Gautheron, C., Reproducibility of Thermal History Reconstruction From Apatite Fission-Track and (U-Th)/He Data. *Geochem Geophys*, 19, 2411-2436, <https://doi.org/10.1029/2018GC007555>, 2018.
- 530
- McDowell, F.W., McIntosh, W.C., and Farley, K.A., A precise ^{40}Ar - ^{39}Ar reference age for the Durango apatite (U-Th)/He and fission-track dating standard. *Chem. Geol.*, 214(3-4): 249-263, doi:10.1016/j.chemgeo.2004.10.002, 2005.
- Naeser, C.W., Zimmermann, R.A. and Cebula, G.T. Fission-track dating of apatite and zircon: An interlaboratory comparison. *Nuclear Tracks* 5, 65-72, 1981.
- 535
- Reiners, P.W., Zircon (U-Th)/He thermochronometry. In: Reiners, P.W., Ehlers, T.A. (Eds.), *Thermochronology, Reviews in Mineralogy and Geochemistry*, 58, 151-179, <https://doi.org/10.2138/rmg.2005.58.6>, 2005.
- Reiners, P.W., and Brandon, M.T., Using thermochronology to understand orogenic erosion. *Ann. Rev. Earth. Planet. Sci.*, 34: 419-466, <https://doi.org/10.1146/annurev.earth.34.031405.125202>, 2006.
- 540
- Reiners, P.W., Farley, K.A., and Hiskes, H.J., He diffusion and (U-Th)/He thermochronology of zircon: initial results from Fish Canyon Tuff and Gold Butte. *Tectonophysics*, 349: 297-308, [https://doi.org/10.1016/S0040-1951\(02\)00058-6](https://doi.org/10.1016/S0040-1951(02)00058-6), 2002.
- Reiners, P.W., and Nicolescu, S., Measurement of parent nuclides for (U-Th)/He chronometry by solution sector ICP-MS. ARHDL Report 1: 1-33, 2007.



- Réveillon, S., Hureau-Mazaudier, Improvements in Digestion Protocols for Trace Element and Isotope Determinations in
545 Stream and Lake Sediment Reference Materials (JSd-1, JSd-2, JSd-3, Jlk-1 and LKSD-1). *Geostandards and Geoanalytical
Research*, 33(3): 397-413, <https://doi.org/10.1111/j.1751-908X.2009.00008.x>, 2009.
- Schmitz, M.D., and Bowring, S.A., U-Pb zircon and titanite systematics of the Fish Canyon Tuff: an assessment of high
precision U-Pb geochronology and its application to young volcanic rocks. *Geochim. Cosmochim. Acta*, 65: 2571-2587,
[https://doi.org/10.1016/S0016-7037\(01\)00616-0](https://doi.org/10.1016/S0016-7037(01)00616-0), 2001.
- 550 Schneider, S., Hammerschmidt, K., Rosenberg, C.L., Gardes, A., Frei, D. and Bertrand, A. U–Pb ages of apatite in the western
Tauern Window (Eastern Alps): Tracing the onset of collision-related exhumation in the European plate. *Earth Planet. Sci.
Lett.*, 418(15): 53-65, <https://doi.org/10.1016/j.epsl.2015.02.020>, 2015.
- Tagami, T., Farley, K.A., Stockli, D.F., (U+Th)/He geochronology of single zircon grains of known Tertiary eruption age.
Earth Planet. Sci. Lett., 207: 57-67, [https://doi.org/10.1016/S0012-821X\(02\)01144-5](https://doi.org/10.1016/S0012-821X(02)01144-5), 2003.
- 555 Tibari, B. Tibari, B., Vacherat, A., Stab, M., Pik, R., Yeghicheyan, D. and Hild, P., An Alternative Protocol for Single Zircon
Dissolution with Application to (U-Th-Sm)/He Thermochronometry. *Geostandards and Geoanalytical Research*, 40: 365-375,
<https://doi.org/10.1111/j.1751-908X.2016.00375.x>, 2016
- Vermeesch, P., RadialPlotter: A Java application for fission track, luminescence and other radial plots. *Radiation
Measurements*, 44: 409-410, 2009.
- 560 Yanga, Y.-H., Wua, F.-Y., Yanga, J.-H., Chew, D.M., Xie, L.-W., Chua, Z.-Y., Zhang, Y.-B. and Huang, C., Sr and Nd isotopic
compositions of apatite reference materials used in U–Th–Pb geochronology. *Chem. Geol.*, 385: 35-55,
<https://doi.org/10.1016/j.chemgeo.2014.07.012>, 2014.
- Yokoyama, T., Makishima, A., Nakamura, E., Evaluation of the coprecipitation of incompatible trace elements with fluoride
during silicate rock dissolution by acid digestion. *Chem. Geol.*, 157: 175-187, [https://doi.org/10.1016/S0009-2541\(98\)00206-](https://doi.org/10.1016/S0009-2541(98)00206-)
565 X, 1999.
- Ziegler, J.F., SRIM-2008 The stopping range of ions in matter. United States Naval Academy, Annapolis, 2008.